Stability of the sectored morphology of polymer crystallites

Jaya Kumar Alageshan, Yashodhan Hatwalne, and Murugappan Muthukumar

Phys. Rev. E **94**, 032506 — Published 26 September 2016

DOI: 10.1103/PhysRevE.94.032506

Stability of the sectored morphology of polymer crystallites

Jaya Kumar Alageshan.,[1] Yashodhan Hatwalne,[1] and Murugappan Muthukumar[2]

[1] *Raman Research Institute, C. V. Raman Avenue, Bangalore 560 080, India*

[2] *Polymer Science and Engineering Department, University of Massachusetts, Amherst, Massachusetts 01003, USA*

(Dated: August 1, 2016)

When an entangled interpenetrating collection of long flexible polymer chains dispersed in a suitable solvent is cooled to low enough temperatures, thin lamellar crystals form. Remarkably, these lamellae are sectored, with several growth sectors that have differing melting temperatures and growth kinetics, eluding so far an understanding of their origins. We present a theoretical model to explain this six-decade old challenge by addressing the elasticity of fold surfaces of finite-sized lamella in the presence of disclination-type topological defects arising from anisotropic line tension. Entrapment of a disclination defect in a lamella results in sectors separated by walls which are soliton solutions of a two-dimensional elliptic sine-Gordon equation. For flat square morphologies, exact results show that sectored squares are more stable than plain squares if the dimensionless anisotropic line tension parameter $\alpha = \gamma_{an}/\sqrt{h_4 K_\phi}$ (γ_{an} = anisotropic line tension, h_4 = fold energy parameter, K_ϕ = elastic constant for two-dimensional orientational deformation) is above a critical value, which depends on the size of the square.

PACS numbers: 81.10.Aj, 81.10.Dn, 82.35.Lr, 83.80.Rs

One of the outstanding phenomena in polymer systems is the ability of a collection of interpenetrating and entangled long flexible polymer chains to organize into crystals upon cooling. The fact that the chains are intermingled among themselves with spatial and dynamical long-ranged correlations before crystallization begins is responsible for the crystallization process being topologically frustrated. Remarkably, crystals do indeed form in spite of such topological frustrations. A rich phenomenology of polymer crystallization has been cultivated over the past seven decades, with numerous sets of experimental data posing challenges for full interpretation [1–13]. As a prominent feature of the phenomenon of polymer crystallization, polymer crystals form as thin lamellae with thickness in the 10 nm range and lateral dimensions in microns or larger. Even under the simplest situation of crystallization from a solution containing sufficiently long and unentangled flexible polymer molecules, single lamellar crystallites have been observed to form spontaneously into a plethora of morphologies [14–25]. The size, shape, and regularity of the crystals depend on their growth conditions such as solvent, temperature, concentration, and rate of growth. For example, flat hexagonal lamellae form when polyoxymethylene is crystallized from bromobenzene [17], whereas flat lozenge shaped lamellae form when polyethylene is crystallized from a mixture of tetrachloroethylene and p-xylene [21]. These single crystals are made of different number of sectors. As another specific example, when polyethylene is crystallized from p-xylene at 70°C, a lamella with four sectors with [110] growth planes forms; at 86°C, a lamella with six sectors, four with [110] planes and two with [100] planes, forms. It is also known that {100} sectors have a lower melting temperature than the {110} sectors. In addition to sectored flat lamellae, other morphologies such as hollow tents, hollow bowls, disks, onion-like, scrolls, and twisted lamellae are also known to form [14–25]. Despite the availability of rich facts, an understanding of polymer single crystal morphology remains as one of the major challenges.

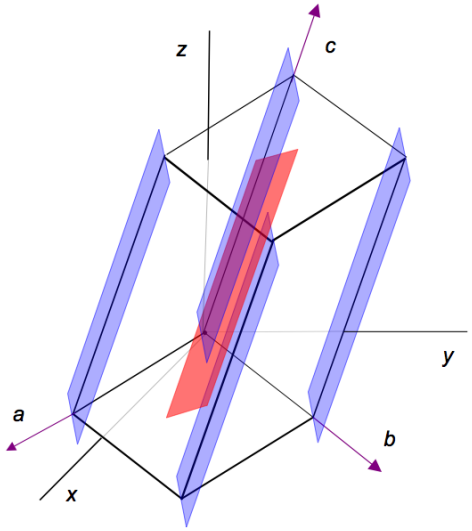

FIG. 1. (Color online) Base-centred orthorhombic unit cell of a crystalline polyethylene lamella. The lamellar normal is along the z- axis. The c- axis of the unit cell is tilted with respect to the z- axis. Shaded strips represent oriented stems formed by all-*trans* configurations. Folds are not shown.

In this paper, we focus on the phenomenon of sectorization in polymer lamellae. Although the sectorization has been known for about six decades [1–8, 14–21, 24, 25], the problem of the structure and stability of sectors observed in lamellar polymer crystallites has hitherto eluded a satisfactory explanation. Why should flat structures with sectors, and bent, tent-shaped structures

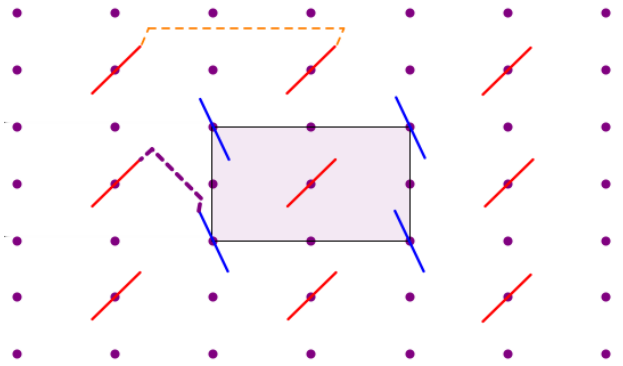

FIG. 2. (Color online) Surface of a polyethylene lamella viewed along the c- axis (see FIG.(1)). Stems, together with their orientation, are indicated by solid lines centred on lattice points. The shaded central region belongs to a unit cell. Two types of folds are represented by dashed lines. The two folds differ in free energy. The thick, dashed fold has the lowest free energy.

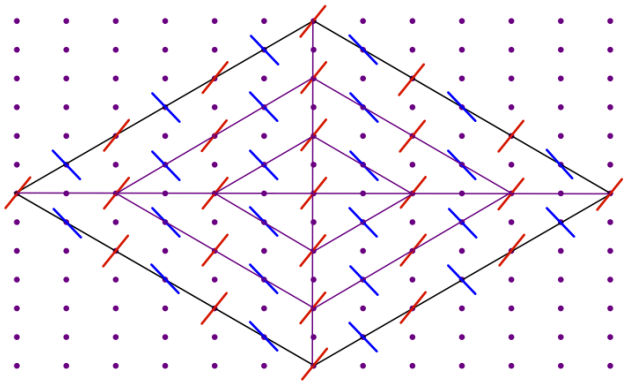

FIG. 3. (Color online) Illustration of an idealized, lozenge shaped, sectored lamella bounded entirely by folds with the lowest free energy. The lamella is divided into four sectors. Folds run along the edges of the three rhombi shown.

that are manifestly deformed be stable? This paper primarily addresses the stability of the flat, sectored morphology of polymer crystallites.

Let us, for concreteness, consider polyethylene crystallites with base-centered orthorhombic symmetry. In the bulk, and along the c- axis of the crystal, the polymer is in all *trans*- conformation, thus forming polymer stems (FIG.(1)). The stems are tilted with respect to the lamellar normal (by about 30° for polyethylene), and fold back into the lamella by switching over from *trans*- to *gauch*- conformation at lamellar surfaces. Folds have preferred orientations with respect to the underlying crystal symmetry. (FIG.2) shows two fold-configurations for polyethylene that have different free energies, schematically representing the 'adjacent reentry' and the 'random switch-board' models [26]. It has been argued that the adjacent reentry configuration (the thick dashed fold denoted in (FIG.2)) is generally of lower free energy [26]. It is important to note that depending upon the symmetry of the underlying crystal lattice the lowest free energy fold configuration can have different orientations. In general, polymer crystallites have different point group symmetries, preferred tilt-, and fold angles. Moreover, in lamellae with a boundary (edge), symmetry considerations allow for folds at the edges favoring a specific orientation with respect to the edge-normal, leading to anisotropy in line tension [27, 28]. Addressing the problem of stability of sectored polymer crystallites is therefore a formidable task. It must be noted that the lateral sizes of the lamellar crystallites are four to five orders of magnitude larger than the atomic dimensions, allowing a continuum description for these crystallites without addressing specific and non universal features of the unit cell [14–25]. In this paper we extract the essential, generic features of flat, lamellar polymer crystallites, and construct a tractable, continuum, phenomenological model for elucidating the structure and stability of sectors.

The model and the mechanism of stability that we propose is primarily based upon the fact that for a finite lamella the ground state fold orientation in the middle of the fold surface cannot possibly be compatible with the most favored orientation of folds throughout the entire boundary of the lamella. This necessarily leads to deformation in the fold-orientation field, and costs elastic free energy. For sufficiently strong anisotropy of line tension, the finite lamella can trap a vortex in the fold-orientation field (a topological defect, also known as a disclination) [29]. Moreover, the fold- field-lines of the disclination (vortex) can split up into sectors separated by wall defects so as to further reduce the free energy cost from anisotropic line tension. In the context of domains of Langmuir monolayers with tilt order, trapping of vortices due to anisotropy of line tension has been studied [30]. A five-armed star defect observed in thin hexatic films with tilt order [31] has been discussed by Selinger and Nelson [32]. This defect has arms (wall defects) of finite, equal lengths that emanate from a disclination. However, anisotropy of line tension plays no role in the stability of the star defect. In this paper we show that intersecting wall defects separate sectors, with a disclination situated at the intersection of walls, and discuss the stability of square-shaped, sectored, planar lamellae in the parameter space.

The proposed two-dimensional, continuum, phenomenological model is described in §1. In §1.1 we discuss the conventional elasticity of the lamella, which is treated as a continuum. §1.2 deals with the energetics of folds. We model the preferred orientations of folds through a simple potential, and the free energy cost for deviations of the fold-field from the preferred orientation by an elastic free energy for the continuum fold-field.

Symmetry-allowed couplings between the displacement field and the fold-field are discussed in §1.3. In addition, there are contributions to the total free energy from (*i*) surface tension of the lamella (either in a solution, or in a melt), (*ii*) line tension from the edges of the lamella, and (*iii*) anisotropic line tension due to folds at the edges. These are considered in §1.4. The potential, and elastic energies of §1.2, as well as the anisotropy of line tension (§1.4) play a crucial role in stabilizing the sectored morphology. As mentioned above, strong anisotropy in line tension is capable of trapping a disclination in the fold-field within a lamella of finite extent. §2 has a simple pedagogical discussion on disclinations and their energetics. In §3 we minimize the total bulk free energy to obtain the equation of equilibrium, and solve it exactly. Typical sketches of the sectored morphology (FIG.(3)) in the literature [22, 23] are consistent with our solution to the equation of equilibrium (FIG.(5)) for the model presented in §1. The solution describes intersecting wall defects in the fold-field. Across the walls, the orientation of fold-field switches over from one minimum of the potential to the other. Walls separate the lamella into sectors, with a disclination of strength +1 in the fold-field (rather than in the displacement field) situated at the point of intersection. This configuration is topologically stable – changing it to that of the ground state involves altering the orientation of the fold-field throughout the lamella. However, since the lamella is of finite extent, it is essential to establish that the sectored morphology is energetically favored over that of the ground state. In §4 we compare the free energy of a lamella in the ground state with that of a sectored lamella, and present a diagram for the region of stability of sectored morphology in parameter space.

§1. ***The model***: In this section we model the free energy costs for deformations in thin lamellar crystals with fold surfaces. We first identify the variables in terms of which the free energy cost for deformations can be described within a continuum description. Since the thickness of crystalline lamellae is much less than their lateral extent they can be treated as two-dimensional plates with appropriately modified elastic moduli, as in the standard theory of thin plates [33]. In the proposed model the lamellar crystal is treated as two-dimensional, with a one-dimensional boundary. Deformations in the plane of the flat lattice are described in terms of a two dimensional displacement field $\boldsymbol{u}(x,y) = (u_x(x,y), u_y(x,y))$, where the xy- plane is the lamellar plane, with lamellar unit normal $\hat{\boldsymbol{n}}$ parallel to the z- axis. The tilt of stems in the undeformed lamellae picks out a special direction in the lamellae. In the lowest free energy, undeformed state, folds at the two fold-surfaces are uniformly aligned. Thus the ground state of a lamella has up-down symmetry. The fold-direction can be characterized by a unit, apolar vector field $\hat{\boldsymbol{n}}_{\rm f} \equiv -\hat{\boldsymbol{n}}_{\rm f}$. Note that we have chosen a unit director (apolar vector) field to describe the folds with the understanding that the free energy cost for stretching or compression of folds is subsumed in the Hookian elasticity.

§1.1. *Hookian elastic free energy*: Crystalline lamellae of polymers have a finite thickness, and have a specific point group symmetry. For example, polyethylene crystallites have orthorhombic symmetry. The elasticity theory of orthorhombic crystals involves nine independent elastic constants. The tilt of stems picks out a special direction in the ground state of the lamellae, and complicates the situation further by contributing to the anisotropy of the elastic tensor. Moreover, changes in the tilt angle, and bending of stems can change the thickness of the lamella.

As mentioned in the introduction to this paper, the phenomenon of sector formation is observed in polymer crystallites having different point group symmetries, and consequently, different numbers of independent elastic constants. To simplify our analysis, and to make it general, we treat the crystalline lamellae as homogeneous and isotropic, and ignore the complications that arise because of specific point group symmetries, tilt- orientations, and thickness variations. For flat, homogeneous, isotropic lamellae, treated as thin plates, the Hookian elastic free energy is given by [33]

$$F_u = \frac{E}{2(1+\sigma)} \int \left[\frac{\sigma}{1-\sigma} u_{ii} u_{jj} + u_{ij} u_{ij} \right] \, \mathrm{d}x \, \mathrm{d}y, \quad (1)$$

where E and σ are two dimensional Young's modulus and Poisson's ratio respectively, the linearised strain tensor $u_{ij} = (1/2)\left[(\partial u_i/\partial x_j) + (\partial u_j/\partial x_i)\right]$; x_i, x_j run over x, y, and repeated indices are summed over. Here, and in all the equations below that involve integration over x- as well as y, the integrals are taken over the entire area of the lamella, with appropriately chosen limits for x and y. In 2-dimensions, $E > 0$, and $-1 < \sigma < 1$ for stability.

§1.2. *Free energy contributions from the fold-field*: Given the crystal structure of the polymer, folds have preferred orientations with respect to the crystal lattice. The two most preferred orientations of folds for polyethylene are shown in the schematic (FIG.(2)). These orientations have different free energies [1]. To simplify the problem at hand we model the simplest possible case, wherein there are two equally preferred, orthogonal fold orientations. The $\hat{\boldsymbol{n}}_{\rm f} \equiv -\hat{\boldsymbol{n}}_{\rm f}$ symmetry then implies that there are four equally preferred, orthogonal directions along which the folds have the least free energy. We have thus chosen this symmetry so as to stabilize a square-shaped lamella. A potential with four equally deep minima;

$$V_{\rm f} = \frac{h_4}{4} \int \cos[4\,\phi(x,y)] \, \mathrm{d}x \, \mathrm{d}y, \quad (2)$$

where $\phi(x,y)$ is the orientation of the fold-director $\hat{\boldsymbol{n}}_{\rm f}(x,y) = (\cos\phi(x,y), \sin\phi(x,y))$ in circular polar co-

ordinates. As is evident from the form of the potential, in the undeformed, ground state of the lamella, ϕ can have orientations given by $p\,\pi/4$, where $p = 1, 3, 5, 7$, so that there are four equivalent ground states, which is consistent with the stipulated symmetry.

Folds can misalign from the preferred orientation. Spatial variations in ϕ cost elastic free energy. We model the elastic free energy of deviations from the preferred orientation by the standard, isotropic, squared gradient elasticity for a two-dimensional deformation in the nematic director [28]

$$E_\phi = \frac{K_\phi}{2} \int (\boldsymbol{\nabla}\phi)^2 \, \mathrm{d}x \, \mathrm{d}y, \tag{3}$$

where K_ϕ is an elastic constant.

§1.3. *Elastic coupling between $\boldsymbol{u}$-, and ϕ- fields* : Couplings between two fields essentially describe the response of one field to changes in the other. The couplings have to be such that the free energy is invariant under symmetry operations of both the fields. The fold- field is apolar, with the symmetry $\hat{\boldsymbol{n}}_\mathrm{f} \equiv -\hat{\boldsymbol{n}}_\mathrm{f}$. The lowest order coupling between the elastic strain u_{ij} and $\hat{\boldsymbol{n}}_\mathrm{f}$ is of the form $(u_{ij} - (1/2)\,\delta_{ij}\,u_{kk})\,n_{\mathrm{f}i}\,n_{\mathrm{f}j}$ [34], where the factor within the brackets represents pure shear deformation (the deviatoric strain, devoid of any hydrostatic compression), the subscripts i, j run over x, y, and repeated indices are summed over. This coupling just means that the response to a shear deformation in the lattice is a change in the orientation of the fold- field (and vice-versa). However, this coupling is not harmonic. We have consistently restricted ourselves to harmonic terms in writing the elastic free energies (1, 3), and we ignore the nonlinear elastic coupling discussed above.

A harmonic coupling between $\boldsymbol{u}$- and ϕ- fields is obtained by appealing to rotational invariance. A rigid, in-plane rotation of the undeformed lamella costs no elastic free energy. Rotation of the crystal lattice is described by the antisymmetric form

$$\delta\omega = \frac{1}{2}\,(\partial_x u_y - \partial_y u_x) = \frac{1}{2}\,\epsilon_{ij}\,\partial_i u_j \tag{4}$$

that is just half the z- component of the curl of $\boldsymbol{u}$. In (4) above, ϵ_{ij} is the totally antisymmetric symbol with $\epsilon_{xy} = -\epsilon_{yx} = 1$, $\epsilon_{xx} = \epsilon_{yy} = 0$. For rigid rotations of the lamella, $\delta\omega$ must equal $\delta\phi$ – the crystal lattice, and the fold-director field $\hat{\boldsymbol{n}}_\mathrm{f}$ must rotate simultaneously by the same amount, so that $\delta\omega = \delta\phi$. The lowest order term that describes the free energy cost for non-rigid, relative rotations is therefore

$$F_{\omega\phi}[\boldsymbol{u}, \delta\phi] = K_{\omega\phi} \int (\delta\omega - \delta\phi)^2 \, \mathrm{d}x \; \mathrm{d}y, \tag{5}$$

where $K_{\omega\phi}$ is the coupling constant. A coupling of this form has been used in the context of nematic elastomers [35, 36]. The free energy (5) is minimized for $\delta\phi \simeq \delta\omega$. In the model we consider, we ignore the coupling (5) for reasons discussed in §2. These have to do with the high free energy cost of a disclination (see §2) in the displacement field, and are of special significance for the tent morphology of polymer crystallites (see §5).

§1.4. *Surface-, and line tension energies*: In a melt or in a solution, the crystallite has a nonzero surface tension free energy

$$E_\mathrm{s} = \sigma \int \mathrm{d}x \, \mathrm{d}y, \tag{6}$$

where σ is the coefficient of surface tension; the lamellar crystallite has two surfaces, the factor of 2 arising from this has been absorbed in defining σ.

The lamella is decorated with folds; it has orientational order. In this context, the line tension at the edges has two contributions. The first contribution

$$E_\mathrm{is} = \gamma \oint \mathrm{d}l, \tag{7}$$

is isotropic, with a coefficient γ, and is the usual line tension that is associated with a surface or a thin film bounded by a curve. The second contribution is special to materials endowed with orientational order, and plays a crucial role in the stability of the sectored morphology. This is the anisotropic line tension that prefers a particular angle between the outward normal to the boundary and the field that describes the orientational order (in this case, the fold-director $\hat{\boldsymbol{n}}_\mathrm{f}$). This contribution to the line tension has the Rapini-Papoular form [27, 28]

$$E_\mathrm{an} = \gamma_\mathrm{an} \oint \sin^2(\phi - \phi_0) \, \mathrm{d}l, \tag{8}$$

where ϕ_0 is the preferred angle of orientation of the fold-field at the boundary. Although nonlinear in form, (8) above is the lowest order contribution to the anisotropic line tension that is consistent with the $\hat{\boldsymbol{n}}_\mathrm{f} \equiv -\hat{\boldsymbol{n}}_\mathrm{f}$ symmetry.

§2. ***Disclinations in two-dimensions – crystalline-, and orientational order***: Before addressing the stability of sectored crystallites it is essential to discuss the structure and energetics of disclinations in two-dimensional crystals, and in fluid membranes with orientational order (such as Langmuir monolayers with tilt order). Let us imagine cutting away a wedge of angle Ω from the center of a thin, homogeneous rubber disk. We then close the angle deficit by sticking together the two newly opened edges (while keeping the disc flat), and allowing the rubber disk to relax. This is the Volterra construction of a disclination [29]. Adding up the incremental angle deficits around any closed loop enclosing the center of the deformed disc yields the total angle deficit Ω. The center of the disk is a singular point (for a quasi-two-dimentional disk). An overall angle deficit corresponds to a positive

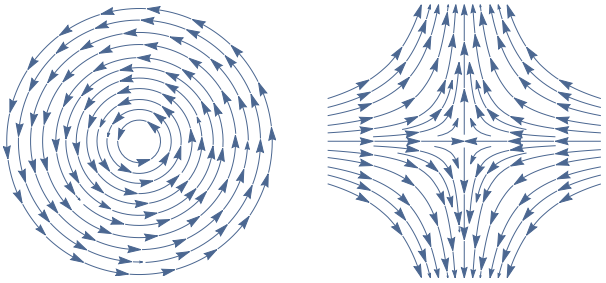

(a) (b)

FIG. 4. (Color online) Elliptic (+1), and hyperbolic (−1) disclinations in the xy-model. Upon traversing an anticlockwise, closed circuit, the vector field rotates in anticlockwise sense through 2π for a +1 disclination, and in clockwise sense through 2π for a −1 disclination..

disclination. Inserting a wedge in a straight cut from the centre of the disk to its boundary leads to an angle excess, which corresponds to a negative disclination. It is important to note that the angle deficit or excess cannot be arbitrary in crystals because of their discrete rotational symmetries.

Disclinations are topological defects (point defects in two-dimensions) and are defined via

$$\oint \mathrm{d}\vartheta = 2\pi s = \Omega, \tag{9}$$

where the integral is taken around a closed curve that encloses the singular disclination point, the angle $\vartheta = \frac{1}{2}\,(\boldsymbol{\nabla}\times\boldsymbol{u})\cdot\hat{\boldsymbol{n}}$, where $\hat{\boldsymbol{n}}$ is the unit normal to the flat crystal, gives the local rotation of the elastic material. The index of the disclination is given by s.

It is straightforward to estimate the free energy cost for a disclination in a crystal. As is evident from the Volterra construction, the displacement field for a disclination is a linear function of the distance from the singular point (at the origin); $\boldsymbol{u} \simeq s\,r$. Suppressing tensorial indices, the elastic free energy of a disclination in a crystal can be schematically written as

$$E_\omega \propto k_{\rm el}\int_0^R (\boldsymbol{\nabla}\boldsymbol{u})^2\, r\,\mathrm{d}r \propto k_{\rm el}\, s^2 R^2, \tag{10}$$

where $k_{\rm el}$ is a typical elastic constant, R is the system size, and we have approximated the elastic free energy density in (1) by $(\boldsymbol{\nabla}\boldsymbol{u})^2 = (\partial_i u_j)^2$. The free energy scales as the area of the system, and is clearly prohibitively costly.

We now move on to disclinations in fluid membranes with orientational order. For concreteness, let us consider the continuum xy-model that has vectorial orientational order described by an angle ψ [29]. For disclinations, $\oint \mathrm{d}\psi = 2\pi s$ (FIG.(4)). This topological condition is satisfied by $\psi = s\arctan(y/x)$. Notice that $\arctan(y/x)$ is just the polar angle in circular polar coordinates. To the harmonic order, the elastic free energy density of the xy-model is proportional to $(\boldsymbol{\nabla}\psi)^2$. Thus the free energy of a disclination is [29]

$$E_\psi \propto k_{xy}\int_\xi^R (\boldsymbol{\nabla}\psi)^2\,\mathrm{d}x\,\mathrm{d}y \tag{11}$$

$$\propto k_{xy}\, s^2 \int_\xi^R \frac{1}{r^2}\, r\,\mathrm{d}r \propto k_{xy}\, s^2 \ln(R/\xi), \tag{12}$$

where k_{xy} is the spin-wave stiffness, R is the system size, and ξ is a cutoff of order intermolecular spacing. In contrast to crystals, the free energy of a disclination in orientational order grows logarithmically with system size.

§3. ***Equation of equilibrium for the ϕ- field, and its solution***: To obtain the equation of equilibrium of the ϕ- field, we minimize the free energy functional $\mathscr{E}[\phi] = E_\phi + V_{\rm f}$ (see (2, 3)). The first variation of $\mathscr{E}[\phi]$ gives

$$\frac{\delta\mathscr{E}[\phi]}{\delta\phi} = -K_\phi\,\nabla^2\phi - h_4\,\sin(4\,\phi) = 0, \tag{13}$$

where $\phi = \phi(x,y)$, and ∇^2 is the Laplacian operator in two dimensions. This equation is a two-dimensional, nonlinear partial differential equation, known as the elliptic sine-Gordon equation [29, 37]. It is well known that the one-dimensional version of this equation admits kink solutions (also referred to as wall- or soliton solutions in condensed matter physics).

To solve this equation in the context of sectors, we first notice that the potential $V_{\rm f}$ has four minima. Next, we observe that setting the preferred angle ϕ_0 for the line tension term (8) (i.e., the angle between $\hat{\boldsymbol{n}}_{\rm f}$ and the outward normal $\hat{\boldsymbol{n}}_b$ to the boundary) equal to $\pi/2$ simplifies the problem for a square-shaped lamella. The folds then prefer to run along the edges of the square. We note that the particular choice $\phi_0 = \pi/2$ is not essential, and the results of calculations that follow do not depend on this choice. This is because the elastic free energy (3) of the ϕ- field is isotropic. Thus, we seek a solution of the Euler-Lagrange equation (13) for a square lamella with the following features: (*i*) two intersecting walls along the diagonals that separate four sectors, and (*ii*) a +1 disclination in the ϕ- field situated at the wall-intersection.

The equation of equilibrium (13) can be solved exactly for the desired configuration discussed above. However, the calculations involved are unwieldy. In what follows we first give the solution, and thereafter present heuristic arguments of a geometric nature that lead to the solution.

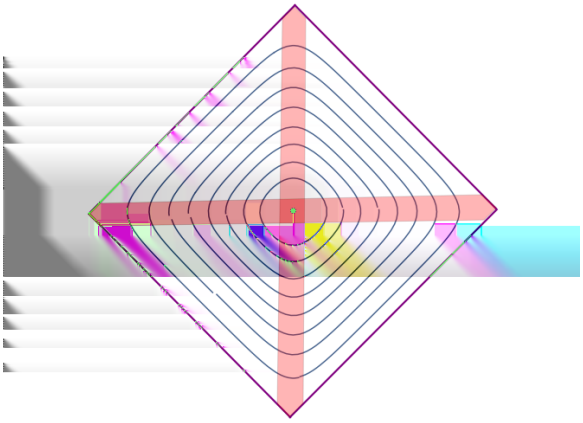

FIG. 5. (Color online) Plot of the solution (14). Lines along rounded squares represent the fold-field. Shaded regions represent the two intersecting walls, with a +1 disclination at the centre. The outermost square is the boundary of the lamella.

The solution is

$$\phi = \arctan\left(\frac{\tanh(y/w)}{\tanh(x/w)}\right) - \frac{\pi}{2}, \tag{14}$$

where the wall width $w = \sqrt{K_\phi/h_4}$. Verification of this solution by direct substitution into the equation of equilibrium (13) also involves complicated mathematical manipulations. Use of symbolic manipulation software packages eases the task. The inverse tangent form for solitonic solutions, and several exact solutions of this form, which are expressible in terms of elementary functions are well known [38, 39]. However, (14) is a special type of vortex solution to the elliptic sine-Gordon equation, describing two intersecting solitons with a +1 vortex (disclination) at their intersection. To our knowledge an exact vortex solution of this form is not previously known. The solution describes two orthogonal walls of width w that intersect at the origin, and split the xy- plane into four sectors. We expect the width w to be of the order of a lattice spacing. The plot of field-lines (or integral curves) of the fold-director $\hat{\boldsymbol{n}}_{\rm f}$ obtained from the solution above is shown in FIG.(5). The origin is a singular point that is a +1 disclination in the ϕ- field. Except for a region of width w near the corners of the square, the fold-field is parallel to the boundary of the square at sufficiently large distances from the origin.

We now turn to the heuristic argument behind the solution (14). Let us consider a hollow, right pyramid with its square base in the xy- plane, and apex on the z-axis. Removal of the base gives a surface with four faces. For such a pyramid, it is easy to see that the projection of the unit normal to the faces onto the xy-plane is perpendicular to the square boundary of the base. Rotating this projected vector field by $\pi/2$ makes it parallel to the square boundary, divides the square into four sectors, and has a +1 disclination at the center of the square. This is close to the field configuration that we are seeking, except that the walls separating the sectors are infinitely sharp; their width is zero. The elliptic sine-Gordon equation (13) has the length scale $w = \sqrt{K_\phi/h_4}$ associated with it. Therefore we need to repeat the procedure described above (projection of the surface normal followed by rotation by $\pi/2$) for a four-sided surface with rounded edges. Such a surface can be modeled by the height function $h(x,y) = a\ln[\cosh(x/w)\cosh(y/w)]$, where a determines slopes of the four faces, and the length scale w determines sharpness of the four edges (FIG.(6)). This surface is described by the position vector $\boldsymbol{R} = (x, y, h(x,y))$. The tangent vectors to the surface are $\boldsymbol{t}_x = \partial_x \boldsymbol{R} = (1, 0, \tilde{a}\tanh\tilde{x})$, and $\boldsymbol{t}_y = \partial_y \boldsymbol{R} = (0, 1, \tilde{a}\tanh\tilde{y})$, where $\tilde{a} = a/w$, $\tilde{x} = x/w$, $\tilde{y} = y/w$, with the unit surface normal given by $\hat{\boldsymbol{n}}_{\rm s} = (\boldsymbol{t}_x \times \boldsymbol{t}_y)/|\boldsymbol{t}_x \times \boldsymbol{t}_y|$. The projection of $\hat{\boldsymbol{n}}_{\rm s}$ in the xy- plane gives the unit vector with components $\hat{\boldsymbol{v}} = (v_x, v_y) = (1/|\boldsymbol{v}|)(-\tilde{a}\tanh\tilde{x}, -\tilde{a}\tanh\tilde{y})$, where the normalization factor $|\boldsymbol{v}| = a\,(\tanh^2\tilde{x} + \tanh^2\tilde{y})^{1/2}$. The angle that $\hat{\boldsymbol{v}}$ makes with the x- axis is given by $\tilde{\phi} = \arctan(v_y/v_x) = \arctan(\tanh\tilde{y}/\tanh\tilde{x})$. However, $\hat{\boldsymbol{v}}$ points towards the origin, and is predominantly along the normal to the square boundary of the projection, whereas the fold-field prefers to be along the edges of the square. Compensating for this undesirable global rotation of $\hat{\boldsymbol{v}}$ by $\pi/2$, we obtain the expression (14), which turns out to be an exact solution to the elliptic sine-Gordon equation.

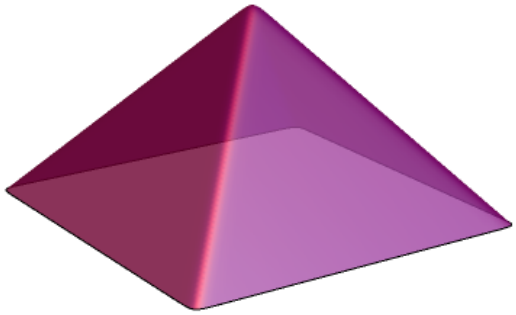

FIG. 6. (Color online) Schematic of the surface $h(x,y) = a\ln[\cosh(x/w)\cosh(y/w)]$.

§4. ***Comparative energetics of distortion-free, and sectored square lamellae***: A "distortion-free" square lamella of finite size does cost free energy due to the anisotropic line tension term, because two opposite edges of the square do not satisfy the condition $\phi_0 = \pi/2$. By comparing square lamellae of the same area, the surface tension term as well as the isotropic line tension term drop out of the problem. The stability of the sectored configuration is clearly determined through the competition between anisotropic line tension-, potential-, and elastic energies. The free energy of the sectored lamella is obtained by substituting the solution for ϕ

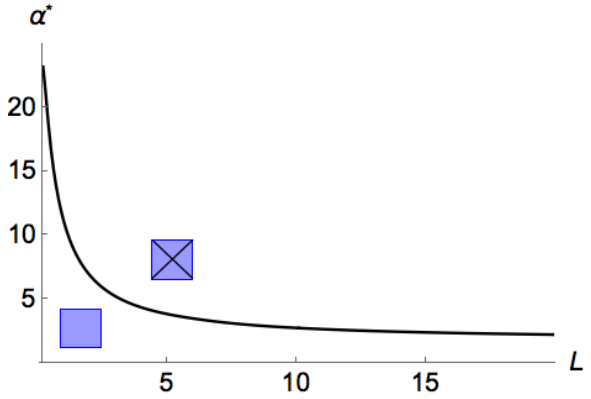

FIG. 7. (Color online) Regions of stability of the undeformed square (below the curve) and the sectored square (above the curve): α^* is the threshold value of $\alpha = w\gamma_{an}/K_\phi$ that separates the regions of stability of the ground state, and sectored configurations. These regions are indicated by an ordinary shaded square, and a crossed, shaded square respectively. L is in units of the wall width w, γ_{an} is the anisotropic line tension, and K_ϕ is the elastic constant for two-dimensional deformation in the nematic director.

(14) in the potential energy (2), the gradient squared elastic free energy (3), and the anisotropic line tension free energy (8).

The integrals involved in the calculation described above cannot be evaluated analytically. Numerical evaluation of the integrals leads to a morphology diagram delineating the relative stability of sectored lamella versus the planar, distortion-free lamella. We identify the key parameter determining the relative stability in terms of the wall width w, the anisotropic line tension $\gamma_{\rm an}$ and the elastic constant K_ϕ. The dimensionless parameter $\alpha = w\gamma_{\rm an}/K_\phi = \gamma_{\rm an}/\sqrt{h_4 K_\phi}$ is the measure of the relative strength of the anisotropic line tension. For every given size of the square there is a threshold value of α, denoted by α^*, that separates the regions of stability of the ground state, and sectored configurations. We measure the dimensionless length L of the side of the square in units of the wall-width w. The dependence α^* on L is shown in FIG.(7). For any given L an increase in $\gamma_{\rm an}$ or a decrease in the product $K_\phi h_4$ leads to stabilization of the sectored configuration. For small sizes of the square, α^* decreases precipitously as the size of the square increases. For large L, α^* decreases weakly with L. We find that the asymptotic value of α^* for large L is about 1.68; however large L may be, the crystallite cannot form sectors unless α^* exceeds this value.

§5. ***Conclusions***: We have constructed a minimal, phenomenological model to address the relative stability of flat, square-shaped, sectored polymer crystallites against undeformed, planar crystallites of the same size and shape. The model uses a combination of the theories of elasticity and topological defects. Three important factors determine the stability of the sectored morphology of polymer crystallites: the orientational potential, the elastic energy, and the anisotropy of line tension. Minimization of the bulk free energy comprising elastic free energy and potential energy of the fold-field leads to the elliptic sine-Gordon equation (13). We obtain an exact solution to this equation (14) that describes the sectored morphology in terms of intersecting wall defects, with a disclination situated at the point of intersection. Wall defects split the crystallite into sectors across which the fold-field switches its orientation by $\pi/2$. We point out that the symmetry-allowed anisotropic line tension term (8) is crucial for stabilizing the sectored morphology of flat polymer crystallites.

An analysis of the solution to the elliptic sine-Gordon equation leads to unique dimensionless parameter $\alpha = \gamma_{\rm an}/\sqrt{h_4 K_\phi}$, where $\gamma_{\rm an}$ is the coefficient of anisotropic line tension, h_4 is the strength of the fold-field potential, and K_ϕ is the elastic coefficient for deformations in the fold-field. For values of α greater than a threshold value α^*, which in turn depends on the edge-size of the square L, sectored lamellae are stabilized.

Returning to the comment made in §1.3 regarding the importance of the $\delta\phi$ - $\delta\omega$ coupling we note the following. If the coefficient $K_{\omega\phi}$ is large enough, the coupling free energy is minimized for $\delta\omega \simeq \delta\phi$, which in turn means that the disclination index s_ϕ of the ϕ- field equals s_u, that of the displacement field $\boldsymbol{u}$. However, symmetry considerations forbid s_ϕ and s_u from taking arbitrary values. Within the planar morphologies considered in this paper, the free energy cost for a disclination in the $\boldsymbol{u}$- field is proportional to the lamellar area R^2. It is known that buckling of a planar lamella with a disclination into one that is cone-shaped mitigates the elastic stress in the lamella; dramatically alleviating the R^2 divergence to a logarithmic divergence $\ln R$ [40]. In the context of disclination induced buckling of lamellae, and the tent morphology of polymer crystallites, the heuristic argument of §3 for obtaining the solution to (13) gains special significance.

Our model is well-suited to account for the large length scales pertinent to experimental observations of sectored morphologies. It does not address the non-universal details ensuing from the crystalline symmetry within ordered domains of the semi-crystalline, sectored morphology with intersecting wall defects and the associated disclination.

Although we have restricted ourselves to square crystallites for the sake of simplicity, our model can be extended to treat other observed planar shapes such as rhombi, and hexagons. It is also of considerable interest to extend our approach to the tent morphology of polymer crystallites – a tent is a "faceted cone", with

a disclination at its apex, and wall defects along its edges.

ACKNOWLEDGEMENT

Acknowledgement is made to the National Science Foundation (Grant No. DMR 1404940).

[1] P. H. Geil, *Polymer Single Crystals* (John Wiley, New York, 1963).
[2] B. Wunderlich, *Macromolecular Physics* (Vol. 1, Academic Press, New York, 1973).
[3] B. Wunderlich, *Macromolecular Physics* (Vol. 2, Academic Press, New York, 1976).
[4] B. Wunderlich, *Macromolecular Physics* (Vol. 3, Academic Press, New York, 1980).
[5] J. D. Hoffman, G. T. Davis and J. I. Lauritzen, in *Treatise in Solid State Chemistry*, Edited by N. P. Hannay, Vol. 3, Chapter 7, (Plenum, New York, 1976).
[6] P. J. Phillips, Polymer Crystals, Rep. Prog. Phys. **53**, 549 (1990).
[7] K. Armistead and G. Goldbeck-Wood, Polymer crystallization theories, *Adv. Polym. Sci.* **100**, 219 (1992).
[8] J. M. Schultz, *Polymer Crystallization* (Oxford University Press, New York, 2001).
[9] M. Muthukumar, *Phil. Trans. R. Soc. Lond.* **A 361**, 539 (2003).
[10] M. Muthukumar, *Adv. Polym. Sci.*, **191**, 241 (2005).
[11] G. Reiter and G. Strobl, *Progress in Understanding of Polymer Crystallization* (Springer, Berlin, 2007).
[12] M. Muthukumar, Shifting Paradigms in Polymer Crystallization, *Lect. Notes Phys.* **714**, 1 (2007).
[13] G. Strobl, *Rev. Mod. Phys.*, **81**, 1287 (2009).
[14] P. H. Geil, *J. Polym. Sci.* **44**, 449 (1960).
[15] D. C. Bassett, F. C. Frank, and A. Keller, *Phil. Mag.* **8**, 1753 (1963).
[16] V. F. Holland and R. L. Miller, *J. Appl. Phys.* **35**, 3241 (1964).
[17] C. A. Garber and P. H. Geil, *Makromol. Chem.* **113**, 236 (1968).
[18] F. Khoury and J. D. Barnes, *J. Res. Nat. Bur. Stands. (U.S.)*, **76A**, 225 (1972).
[19] F. Khoury and J. D. Barnes, *J. Res. Nat. Bur. Stands. (U.S.)*, **78A**, 95 (1974).
[20] J. D. Barnes and F. Khoury, *J. Res. Nat. Bur. Stands. (U.S.)*, **78A**, 363 (1974).
[21] J. C. Wittman and B. Lotz, *J. Polym. Sci. Part B: Polym. Phys.* **23**, 205 (1985).
[22] S. J. Organ and A. Keller, *J. Mater. Sci.* **20**, 1571 (1985).
[23] D. C. Bassett, R. H. Olley, and I. A. M. Al Reheil, *Polymer*, **29**, 1539 (1988).
[24] A. S. Vaughan, *J. Mat. Sci.*, **28**, 1805 (1993).
[25] R. M. Briber and F. Khoury, *J. Polym. Sci. Part B: Polym. Phys.* **31**, 1253 (1993).
[26] *Faraday Discussions of the Chemical Society* **N0.68**. Organization of Macromolecules in the Condensed State, (The Faraday Division, Royal Society of Chemistry, London, 1979).
[27] A. Rapini and M. Papoular, *J. Phys. (Paris) Colloq.* **30**, 54 (1969).
[28] P. G. de Gennes and J. Prost, *The Physics of Liquid Crystals* (Clarendon Press, Oxford, 1993).
[29] P. M. Chaikin and T. C. Lubensky, *Principles of Condensed Matter Physics* (Cambridge Univ. Press, 1995).
[30] D. Pettey and T. C. Lubensky, *Phys. Rev. E* **59**, 1834 (1999), and references therein.
[31] S. B. Dierker, R. Pindak and R. B. Meyer, *Phys. Rev. Lett.* **56**, 1819 (1986).
[32] J. V. Selinger and D. R. Nelson, *Phys. Rev. A* **39**, 3135 (1989).
[33] L. D. Landau and E. M. Lifshitz, *Theory of elasticity* (Pergamon Press, Oxford, 1986).
[34] D. R. Nelson and B. I. Halperin, *Phys. Rev. B* **21**, 5312 (1980).
[35] O. Stenull and T. C. Lubensky, *Phys. Rev. E* **69**, 021807 (2004).
[36] M. Warner and E. M. Terentjev, *Liquid Crystal Elastomers* Clarendon Press, Oxford, 2007.
[37] J. Frenkel and T. Kontorova, *Izv. Acad. Nauk SSSR, Seria Fizicheskaya* **1**, 137 (1939).
[38] See T. Aktosun, F. Demontis and C. van der Mee, *J. Math. Phys.* **51**, 123521 (2010), and references therein.
[39] See V. E. Sinitsyn, I. G. Bostrem and A. S. Ovchinnikov, *J. Phys. Cond. Matt.* **16**, 3445 (2004), and references therein.
[40] H. S. Seung and D. R. Nelson, *Phys. Rev. A* **38**, 1005 (1988).